Journal of Photochemistry and Photobiology A: Chemistry 206 (2009) 93–101

Contents lists available at ScienceDirect

Journal of Photochemistry and Photobiology A: Chemistry

journal homepage: www.elsevier.com/locate/jphotochem

Photophysical and photochemical properties of the T_1 excited state of thioinosine

G. Wenska[a,*], J. Koput[a], G. Burdziński[b], K. Taras-Goslinska[a], A. Maciejewski[a,c]

[a] Faculty of Chemistry, A. Mickiewicz University, Grunwaldzka 6, 60-780 Poznań, Poland
[b] Faculty of Physics, A. Mickiewicz University, Umultowska 85, 61-614 Poznan, Poland
[c] Center for Ultrafast Laser Spectroscopy, A. Mickiewicz University, Umultowska 85, 61-614 Poznan, Poland

ARTICLE INFO

Article history:
Received 3 April 2009
Received in revised form 11 May 2009
Accepted 22 May 2009
Available online 30 May 2009

PACS:
33.50.–j
71.15.–m
87.15.–v
82.39.Pj
82.50.Hp

Keywords:
Thione
Thiol
Tautomer
Thioinosine
Triplet state
Singlet oxygen

ABSTRACT

UV–VIS absorption, circular dichroism, room-temperature emission and nanosecond transient absorption measurements as well as steady-state photochemical methods were used to determine the photophysical and photochemical properties of the lowest excited triplet state (T_1) of 2′,3′,5′-tri-O-acetyl-thioinosine (6-thiopurine 2′,3′,5′-tri-O-acetyl-riboside, TI) in acetonitrile (ACN) solutions. The experimental data were supplemented by ab initio quantum chemical calculations on 9-methyl-6-thiopurine (Me^9TP), a model molecule for the nucleoside. The ground state tautomeric structures were computed at the MP2/aug-cc-pVTZ level of theory, and the CPCM model was used for an evaluation of the solvent effects. The results show that, in contrast to the gas phase, the thione tautomer is about 6 kcal/mol more stable than the thiol form in ACN solution. The predominance of the thione tautomer of TI in solution was confirmed by the good agreement between the measured UV absorption spectrum of TI and the calculated singlet electronic transitions and intensities of the thione form of Me^9TP. In addition there was a very close resemblance between the experimental UV spectrum of TI and that of its derivative fixed by the methyl group in the thione tautomeric form. The T_1 state of TI was characterized by its energy, phosphorescence (ϕ_p^0), nonradiative process (ϕ_{nr}), photochemical reaction (ϕ_{pch}) quantum yields, intrinsic lifetime (τ_T^0), rate constants of self-quenching (k_{sq}), phosphorescence (k_p), and nonradiative processes (k_{nr}). The rate constants for the quenching of the T_1 state of TI by standard triplet quenchers (O_2, KI) and by common constituents of nucleic acids (pyrimidine and purine nucleosides) were also determined. The results show that the T_1 state of TI exhibits the properties typical of the $^3(\pi\pi^*)$ states of aromatic thiocarbonyl compounds, i.e. weak room-temperature phosphorescence ($\phi_p^0 = 2 \times 10^{-4}$), fast self-quenching process ($k_{sq} = 7.4 \times 10^9\ M^{-1}\ s^{-1}$) and high reactivity towards O_2 ($k_q \sim 6.8 \times 10^9\ M^{-1}\ s^{-1}$). Mechanistic studies of the steady-state photolysis of TI in air-equilibrated ACN solutions revealed that TI acts as a sensitiser and an acceptor of singlet oxygen.

1. Introduction

Ribosides and deoxyribosides of thiopyrimidines (4-thiouridine, 4-thiothymidine) and thiopurines (thioinosine, thioguanosine) are important derivatives of nucleic acid components because of their widespread applications in molecular biology and pharmacology [1–5]. The compounds are interesting objects of photochemical studies for two main reasons. First, the nucleosides absorb the light in the UVA spectral region, in contrast to the common non-sulfur-containing nucleic acid components. Therefore they can be selectively excited when present in biological systems, and their molecules in the electronically excited states are regarded as reactive precursors in photochemical reactions involving other cell components. These photochemical reactions are the basis of a crosslinking technique frequently applied in the studies of three-dimensional structures of nucleic acids and their complexes with proteins [1–3]. It has been also found that the nucleosides of 4-thiopyrimidines and thiopurines incorporated into cellular DNA induce phototoxic effects upon UVA irradiation of cells [2,6–8]. These effects exerted by low doses of radiation are of promising therapeutic value. Thus, the knowledge of the photochemical and photophysical properties of thiopyrimidine and thiopurine nucleosides is prerequisite for a proper interpretation of the experimental data obtained for more structurally complex biological systems and for an understanding the photoreaction mechanisms at the molecular level. Second, thiopurines and thiopyrimidines in their thione tautomeric form are representatives of a family of aza-heterocyclic thiocarbonyl compounds. While the spectral, photophysical and photochemical properties of aliphatic and aromatic thioketones in several excited triplet (T_1, T_2) and singlet states (S_1, S_2) [9–11] have been well recognized, those of aza-heterocyclic thiones remained unknown or confined to the lowest T_1 state.

* Corresponding author. Tel.: +48 61 829 13 51; fax: +48 61 865 80 08.
E-mail address: gwenska@amu.edu.pl (G. Wenska).

1010-6030/$ – see front matter © 2009 Elsevier B.V. All rights reserved.
doi:10.1016/j.jphotochem.2009.05.021

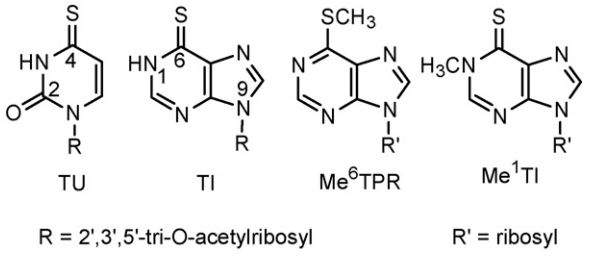

Chart 1.

Among the sulfur analogs of common nucleosides only thiopyrimidine nucleosides, in particular 4-thiouridine (TU, Chart 1) has been subjected to extensive studies both experimental and theoretical [1,2,12–19]. The nucleoside TU and other N(1)-substituted derivatives of 4-thiouracil in their ground states (S_0) were shown to exist exclusively as their thione tautomers, irrespective their environment. The most important deactivation pathways of the T_1 state of TU were identified, and the rate constants of the photophysical processes were determined in several solvents [2,14–16].

To our knowledge no attention in this respect has been paid so far to the thiopurine nucleosides. As a continuation of our interest in the sulfur-containing modified nucleosides, we have undertaken the studies of the spectral, photophysical and photochemical properties of thioinosine. The acetylated nucleoside, i.e. 2′,3′,5′-tri-O-acetyl-9-(β-D-ribofuranosyl)-6-thiopurine, (TI, Chart 1) instead of its non-acetylated counterpart has been used in these studies because of the much better solubility of the former in acetonitrile (ACN), which was the solvent used throughout this work. The structure of the compound is presented in Chart 1.

In this paper we report the results of the investigations performed by experimental and quantum chemical methods. The main goals of the present work are the spectral characterization of TI in its lowest energy excited triplet state (T_1) and to identify the relevant processes both photophysical and photochemical of its excited state decay.

2. Experimental

2.1. Materials

Thioinosine (Aldrich), methylene blue (Aldrich), rose bengal (Windsor Lab, Ltd.), nitroblue tetrazolium (Aldrich), 2′,3′,5′-tri-O-acetyl-guanosine (Aldrich) and acetonitrile (ACN, Uvasol Merck) were used as received. The acetylated nucleosides: 2′,3′,5′-tri-O-acetyl-inosine [20], 2′,3′,5′-tri-O-acetyl-uridine, 3′,5′-di-O-acetyl-thymidine [21], 9-methyl-adenine [22], 2′,3′,5′-tri-O-acetyl-4-thiouridine [23], 9-(β-D-ribofuranosyl)-1-methyl-6-thiopurine, 6-methylthio-9-(β-D-ribofuranosyl)-purine, [24] and 9-(2′,3′,5′-tri-O-acetyl-β-D-ribofuranosyl)-6-thiopurine [25] were synthesized as described previously. The latter compound was purified by repeated crystallization (at least twice) from acetone–water mixture. The purity of the compound for spectral measurements was checked by HPLC.

Bis[9-(2′,3′5′-tri-O-acetyl-β-D-ribofuranosyl-6-purinyl) disulfide (**3**) was obtained by the procedure similar to that described previously for deacetylated nucleoside [26]. The compound was isolated from a reaction mixture by preparative HPLC. Selected spectral data are given below. The ^{1}H and ^{13}C chemical shifts (δ) are in ppm relative to TMS as the internal standard. Atom numbering for NMR data is shown in Scheme 1.

UV (H_2O): λ_{max} = 288 nm, ε_{max} = 26,900 M^{-1} cm^{-1}. ^{1}H NMR ($CDCl_3$, δ ppm) 8.71 (s, 1, 2-H), 8.22 (s, 1, 8-H), 6.23 (d, 1, 1′-H), 5.96 (t, 1, 2′-H), 5.65 (m, 1, 3′-H), 4.41 (m, 3, 4′-H and 5′-H), 2.14 (s, 3, CH_3), 2.12 (s, 3, CH_3), 2.08 (s, 3, CH_3). ^{13}C NMR ($CDCl_3$, δ ppm) 170.25, 169.51, 169.27, 157.74, 152.50, 149.02, 142.18, 132.34, 86.53, 80.44, 73.02, 70.52, 62.91, 20.71, 20.47, 20.33. ESI-MS *m*/*z*: 819.16 [M + H$^+$].

2.2. Methods

2.2.1. Instrumentation

UV absorption and steady-state emission spectra were recorded at room temperature in 1 cm × 1 cm quartz cells using a CaryBio spectrophotometer and an LS 50B Perkin Elmer spectrofluorimeter, respectively. The emission spectra were corrected for instrumental distortion. Phosphorescence quantum yield was determined using quinine sulfate in 0.05 M H_2SO_4 as a reference (ϕ = 0.52) [27]. HPLC was performed on a Waters 600 E instrument equipped with a Waters 991 Photodiode Array Absorption detector and a Waters 470 Scanning Fluorescence Detector. The HPLC analyses were carried out on a reversed-phase column (X-Terra RP18, 3.5 mm, 4.5 mm × 150 mm) using a gradient H_2O–ACN (4:1) → (15 min) H_2O–ACN (1:4). The ^{1}H and ^{13}C NMR spectra were measured at 300 MHz (^{1}H) and 75 MHz (^{13}C) using a Varian Unity spectrometer. MS spectra (electrospray) were recorded on an AMD Intectra Model 604 or a Bruker MicroTOF Q instruments. The circular dichroism spectrum was measured using a JASCO J-580 dichrograph.

2.2.2. Steady-state irradiation and quantum-yield determination

Solutions (2.5 mL) of TI ($c \sim 0.1$ mM) in ACN in a quartz cell (l = 1 cm) were irradiated using a 200 W high pressure mercury lamp equipped with a pyrex ($\lambda > 300$ nm) or an interference filter (λ = 313 nm). For irradiation in the absence of oxygen, solutions were deaerated by bubbling with argon; otherwise the solutions were irradiated in an open-to-air cell (air-equilibrated). In dye sensitized photoreactions, solutions containing methylene blue or rose bengal (c = 0.05 mM) and TI ($c \sim 0.07$–0.1 mM) were irradiated in air-equilibrated ACN solutions at $\lambda > 400$ nm. Irradiations (λ = 313 nm) in the presence of nitroblue tetrazolium were performed using solutions containing TI (c = 0.2 mM) and the indicator (c = 0.05 mM) in air-equilibrated ACN. The photoreactions were followed by measuring the absorbance in the visible region ($\lambda \sim 500$ nm). The concentrations of substrate and photoproducts were determined by HPLC analysis. The photoproducts **2** and **3** were identified by a comparison of the HPLC peak retention time, UV–VIS absorption and MS spectra with those of authentic, synthesized samples. The photoproducts **1a** and **1b** were identified as sulfinic and sulfonic acid, respectively, on the basis of UV and ESI-MS spectra (**1a**: λ_{max} = 271 nm, 345 nm in ACN–H_2O; **1b**: λ_{max} = 271 nm, for $C_{16}H_{17}N_4O_{10}S$ [M−H$^+$] calc. 457.0664 *m*/*z*, found 457.0763. The total yield of **1a** and **1b** was determined following the quantitative transformation of HPLC isolated photoproducts into 2′,3′,5′-tri-O-acetyl-inosine in 0.05 M HCl at room temperature [28]. For quantum-yield determinations the samples were irradiated at λ = 313 nm to <25% conversion of the substrate, and the substrate disappearance was measured by HPLC. Uranyl oxalate was used as the actinometer [29].

2.2.3. Transient absorption spectroscopy

A detailed description of the experimental set-up and data analysis has been described previously [30]. The Q-switched Nd:YAG laser (Continuum Surelite II) generated 8 ns (fwhm), 1 mJ pulses at 355 nm with a repetition rate of 0.5 Hz. The transients were monitored with a pulsed 150 W xenon arc lamp (Applied Photophysics). The transmitted probe light was dispersed by a monochromator (6 nm spectral resolution, Acton Research SpectraPro 300i) and detected by a photomultiplier tube (R928 Hamamatsu) coupled to a digital oscilloscope (Tektronix TDS 680 C). The output signal was analyzed by a PC using a home-made program written in the LabView 4.1 environment. All experiments were carried out in a

rectangular quartz optical cell (1 cm × 1 cm). The solutions were deaerated for about 15 min prior to each experiment with an argon gas flow to remove traces of O_2.

2.2.4. Theoretical calculations

The equilibrium structures and energetics of the 9-methyl-6-thiopurine tautomeric forms in their ground electronic states were determined using the spin restricted Møller–Plesset second-order method, MP2 [31] in conjunction with the augmented correlation-consistent basis sets, aug-cc-pVnZ, of double (n = D) and triple-zeta (n = T) quality [32,33]. To estimate the electron correlation effects beyond the MP2 method, single-point calculations were performed for the MP2/aug-cc-pVTZ equilibrium structures using the coupled-cluster method, CCSD(T) [34], in conjunction with the aug-cc-pVDZ basis set. The vibrational zero-point energies were calculated within the harmonic approximation at the MP2/aug-cc-pVDZ level of theory. The electronic excited state energies and transition oscillator strengths were determined using the configuration interaction methods, CIS and CIS(D) [35,36], in conjunction with the aug-cc-pVTZ basis set. In the CIS approach, the calculations included all singly excited configurations within the valence active space. The CIS(D) method includes additionally a second-order perturbational correction to the CIS excitation energy and, therefore, it is analogous to the MP2 approach for the ground electronic state. The solvent effects were accounted for within the CPCM model [37] at the CIS/aug-cc-pVTZ level. The calculations were performed using the Gaussian 03 package [38].

3. Results and discussion

3.1. Ground state tautomeric structure

In order to determine the ground state (S_0) tautomeric structure of TI (thione vs. thiol) in ACN solution, the relative stability of the tautomers was computed taking into account the solvent effect. All ab initio calculations were performed for the 9-methyl-6-thiopurine molecule (Me^{9}TP, Chart 2) which contains a methyl group instead of a ribosyl substituent at the N(9) position of the purine ring. The structures of the Me^{9}TP tautomers are displayed in Chart 2. In analogy to the previous study on 6-thiopurine by Lapinski et al. [39], thione and two conformers of thiol with a cis and trans orientation of the hydrogen atom of the SH group relative to the N(1) atom of the purine ring were considered.

The predicted relative energies (with respect to the thione form) of the three species of interest are given in Table 1. The total energy quoted is the sum of the total electronic energy in vacuo or in solution calculated at the MP2/aug-cc-pVTZ level of theory, the vibrational zero-point energy, and the CCSD(T) vs. MP2 correction (see Theoretical calculations in the Experimental section for details). The latter two quantities are assumed to be the same in vacuo and in solution. For the isolated Me^{9}TP molecule, the thiol trans form is predicted to be the lowest in energy. It is interesting to note that this is largely due to the substantial difference in the vibrational zero-point energies of the thione and thiol forms. Considering the dependence of the relative energies upon the size of one-particle basis set and the neglected high-order electron correlation and vibrational anharmonic effects, the predicted relative total energies are believed to be accurate to ±1 kcal/mol. Therefore, isolated Me^{9}TP molecules exist at room temperature largely as the thiol trans form. The abundance ratio of the thione, thiol cis, and thiol trans forms is estimated from the Boltzmann factors to be 0.01:0.04:1.[1] The situation changes dramatically for Me^{9}TP molecules embedded in the ACN solvent. Inclusion of the solvent effect within the conductor-like polarizable continuum model, CPCM, increases substantially the relative total energies of the thiol forms. As a result, it is the thione form which is predicted to be the most stable form in solution. Because differences in the total energies of solvated molecules are large (see Table 1), the thione form is predicted to be the very most abundant tautomeric form of Me^{9}TP in solution. For room temperature, the abundance ratio of thione, thiol cis, and thiol trans forms in ACN is estimated to be $1:3 \times 10^{-5}:2 \times 10^{-5}$. The large differences in the total energies of solvated molecules can be attributed to large differences in the total dipole moments of the tautomeric forms presented in Chart 2. At the HF/aug-cc-pVTZ level of theory, the total electric dipole moments of the thione, thiol cis and thiol trans forms are calculated to be 7.4, 4.0, and 5.1 Debye, respectively. Because the solvation energy depends approximately on the square of the dipole moment, the solvation energy of the thione form is (in absolute value) a factor of about 2 larger than the thiol cis and thiol trans forms. In fact, the solute-solvent interaction energies were calculated at the HF/aug-cc-pVTZ level to be −32.5, −15.4, and −14.2 kcal/mol for the forms thione, thiol cis and thiol trans, respectively.

Table 1
Relative energies (in kcal/mol) of the thiol vs. thione[a] tautomers of Me^{9}TP.

	thiol *cis*	thiol *trans*
E (MP2/aug-cc-pVDZ)[b]	2.01	1.08
E (MP2/aug-cc-pVTZ)[b]	1.22	0.18
ZPE[c]	−2.38	−2.27
ΔE (CC-MP)[d]	−0.81	−0.71
Total (isolated molecules)	**−1.97**	**−2.80**
Energy in solution[e]	8.86	8.91
Nonelectrostatic terms	0.58	0.65
Total (molecules in solution)	**6.25**	**6.58**

[a] The thione tautomer energy is taken as zero.
[b] The total electronic energy calculated at the given level of theory.
[c] The vibrational harmonic zero-point energy calculated at the MP2/aug-cc-pVDZ level.
[d] The difference between the total electronic energies calculated using the CCSD(T) and MP2 methods, both with the aug-cc-pVDZ basis set.
[e] The total electronic energy calculated at the MP2/aug-cc-pVTZ level using the CPCM model for the ACN solvent.

3.2. Spectral characterization of the excited states of TI

The absorption spectrum of TI in ACN is presented in Fig. 1. In the spectral region 220–450 nm the compound exhibits an intense (ε_{max} = 22,500 M^{-1} cm^{-1}) band with a maximum at λ_{max} = 325 nm. The high intensity of the band indicates that it is associated with a $\pi \rightarrow \pi^*$ electronic transition. A shoulder with an inflection point at λ = 378 nm ($\varepsilon \sim 90$ M^{-1} cm^{-1}) was observed at the red-end of the

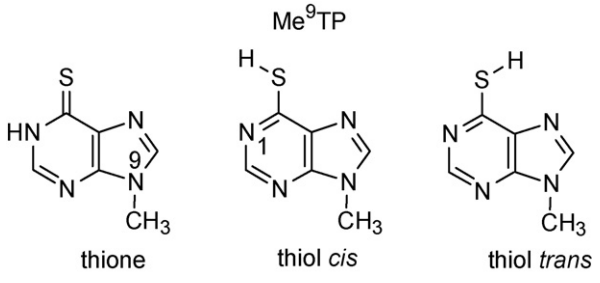

Chart 2.

[1] Because the vibration-rotation properties of the three species are similar, the thermal corrections to the total energy are expected to be nearly the same. In fact, the thermal corrections (differences between the Gibbs free energy at 298 and 0 K) are calculated at the MP2/aug-cc-pVDZ level to be 22.1, 22.2, and 22.2 kcal/mol for the thione, thiol cis, and thiol trans tautomers, respectively.

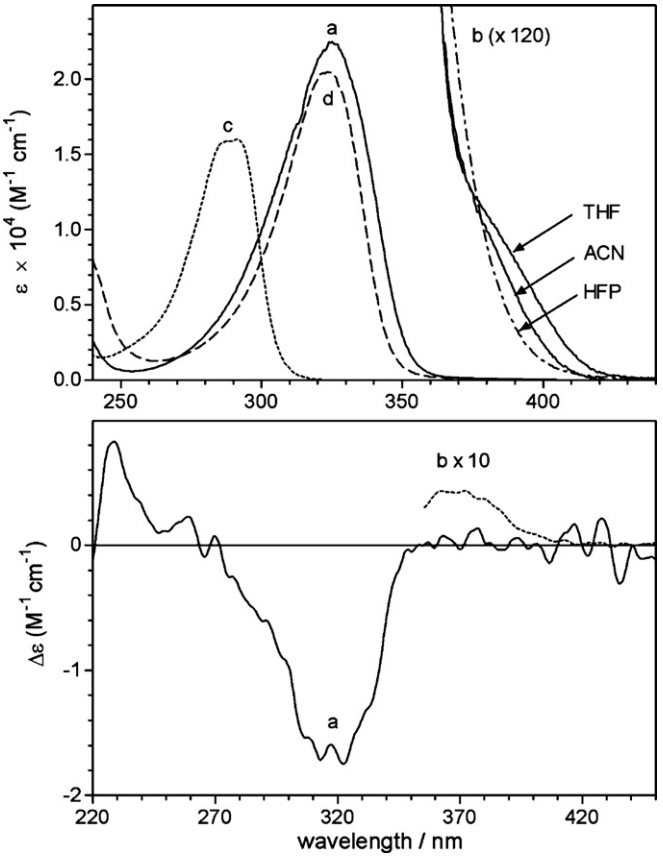

Fig. 1. Upper panel: the UV absorption spectra of: (a) TI, (c) Me[6]TPR, (d) Me[1]TI in ACN and (b) the $S_0 \rightarrow S_1$ band of TI in ACN, tetrahydrofuran (THF) and hexafluoro-2-propanol (HFP). Lower panel: CD spectrum of TI in ACN. The spectra (a), (c) and (d) were measured using the solutions at the concentrations 0.3–0.8 × 10^{-4} M; the spectra (b) were recorded using the concentrations 0.2–2.5 × 10^{-3} M.

intense absorption band when the UV–VIS absorption spectrum was measured using a more concentrated solution (c_{TI} > 0.2 mM). This very weak long-wavelength absorption did not appear as a separate band even in less polar aprotic solvents (valeronitrile, ethyl acetate, tetrahydrofuran), but the distinct bathochromic shift of the shoulder in less polar solvents was observed. The weak shoulder was not seen in the spectrum measured in hexafluoro-2-propanol, which acts as a good H-bond donor. The hydrogen-bonding solute-solvent interaction increases the $n \rightarrow \pi^*$ transition energy and shifts the band under strong π,π^* absorption. The low intensity and solvent effect suggest that the weak absorption in the long-wavelength spectral region originates from an $n \rightarrow \pi^*$ electronic transition. The two lowest energy $n \rightarrow \pi^*$ and $\pi \rightarrow \pi^*$ singlet electronic transitions were detected in the CD spectrum of TI. They appear as a weak positive peak at $\lambda \sim 360$ nm and somewhat stronger negative peak at $\lambda \sim 320$ nm, respectively (Fig. 1). The physical basis for the CD curve is an electronic transition in an optically active chromophore. The purine and pyrimidine bases are not optically active because the molecules are achiral. The optical activity of purine and pyrimidine in nucleoside results from interaction between the base transition dipole and chiral sugar residue.

The UV absorption spectroscopy was found to be suitable for distinguishing between the thione and thiol tautomeric forms of TI. The absorption spectra of the compounds Me[1]TI and Me[6]TPR (Chart 1), which are the models of the fixed thione and thiol tautomers of TI, respectively, are presented in Fig. 1. The close resemblance of the spectra of Me[1]TI and TI is evidence that the latter compound exists primarily as the thione tautomer in ACN solutions.

Table 2
The vertical singlet and triplet electronic state energies (E, in cm^{-1}) and $S_0 \rightarrow S_n$ transition oscillator strengths (f) for the thione form of Me[9]TP.

Isolated molecules			Solvent shift	Molecules in ACN solution	
Symmetry	E^a	f	ΔE^b	E^c	f
$S_0 \rightarrow S_n$					
$^1A''$ (n,π*)	26,000	0.000	+5900	31,900	0.000
$^1A'$ (π,π*)	32,600	0.580	−200	32,400	0.738
$^1A'$ (π,π*)	36,200	0.233	+3200	39,400	0.170
$^1A''$ (n,π*)	41,500	0.016	+3300	44,800	0.054
$^1A'$ (π,π*)	44,900	0.015	+2600	47,500	0.049
$^1A''$ (n,π*)	45,500	0.000	+4600	50,100	0.023
$^1A'$ (π,π*)	45,800	0.052	+3600	49,400	0.119
$S_0 \rightarrow T_n$					
$^3A'$ (π,π*)	25,000		−1000	24,000	
$^3A''$ (n,π*)	25,300		+6600	31,900	
$^3A'$ (π,π*)	32,700		+2100	34,800	
$^3A'$ (π,π*)	41,600		−800	40,800	

[a]Calculated at the CIS(D)/aug-cc-pVTZ level. [b]Calculated at the CIS/aug-cc-pVTZ level using the CPCM model for the ACN solvent. [c]The energy of an isolated molecule (E) plus the solvent shift (ΔE)[b].

The results obtained from the experimental absorption spectrum of TI were compared with the computed energies, oscillator strengths and symmetry of singlet electronic transitions of the thione form of Me[9]TP. The calculations were performed for isolated molecules and for molecules in ACN solution. The excited state energies and transition oscillator strengths were determined for the ground state equilibrium structures using the configuration interaction methods, CIS and CIS(D), both in conjunction with the aug-cc-pVTZ basis set. The solvent effects were accounted for within the CPCM model at the CIS/aug-cc-pVTZ level of theory. The excited state energies were determined for the ground state equilibrium structures in solution, thus taking into account both direct and indirect solvent effects. The results are given in Table 2. The calculations predict that the $S_0 \rightarrow S_1$ electronic transition of the isolated Me[9]TP (thione) molecule is of the n,π* character and that its vertical energy is 6600 cm^{-1} lower than the vertical transition energy to the second excited state S_2 (π,π*). In ACN solution, the energy of the first excited singlet state increases considerably (the solvent shift ΔE = +5900 cm^{-1}), while the vertical transition energy to the S_2 state remains almost unchanged (the solvent shift ΔE = −200 cm^{-1}).

An unexpectedly large shift of the $n \rightarrow \pi^*$ transition towards higher energy in the aprotic, polar solvent (ACN) is due to the destabilization of the S_1 excited state. The Me[9]TP molecule in the S_1 excited state is less polar than in the S_0 state (the total dipole moment is calculated to be 7.4 and 3.4 D in the S_0 and S_1 states, respectively) as a result of redistribution of electronic density from the sulfur atom to the purine ring atoms. The effective atomic charges in the ground state S_0 as well as in the excited states S_1 and S_2 calculated for the thione form of the Me[9]TP molecule in ACN solution are given in Supplementary material section. The calculations accurately predict the location of the $S_0 \rightarrow S_2$ band maximum in the experimental spectrum of TI (a 1600 cm^{-1} energy difference, see Table 2 and Fig. 1). The agreement between the calculated vertical energy of the $S_0 \rightarrow S_1$ transition and the observed location of the lowest weak absorption band in the experimental spectrum is reasonable. In the observed CD spectrum of TI, the maximum of the weak band (λ = 360 nm) lies midway between the $S_0 \rightarrow S_1$ vertical transition energies calculated for an isolated and solvated Me[9]TP molecule (Table 2 and Fig. 1).

The important conclusions from the results in Table 2 concerning the triplet states are that the T_1 excited state of Me[9]TP should have a π,π* configuration regardless the solvent polarity and that the intersystem crossing S_1 (n,π*) ∼ > T_1 (π,π*) should be a fast pro-

cess according to the El-Sayed rule [40]. Note that the lowest excited singlet and triplet states of the n,π* character are predicted to have nearly the same energy, whereas those of the π,π* character are far apart, with the difference in vertical transition energies amounting to as much as 8000 cm^{-1}. This is consistent with singlet–triplet splittings of the lowest n,π* and π,π* states observed in aromatic thioketones [41]. Due to the size of Me^9TP, it is not feasible at present to calculate the adiabatic energy of the T_1 state at the CIS(D)/aug-cc-pVTZ level of theory. Therefore, the difference between the vertical and adiabatic energies of the T_1 state was estimated using the HF and CIS methods. The equilibrium structure of Me^9TP in its ground electronic state was calculated at the HF/aug-cc-pVTZ level, then the $S_0 \rightarrow T_1$ vertical transition energy was calculated at the CIS/aug-cc-pVTZ level. On the other hand, the equilibrium structure of Me^9TP in the T_1 state was determined at the CIS/aug-cc-pVTZ level, thus yielding the $T_1 \rightarrow S_0$ vertical transition energy. The difference between the $T_1 \rightarrow S_0$ and $S_0 \rightarrow T_1$ vertical transition energies of Me^9TP was determined in this way to be −2300 cm^{-1}. Because the calculated value is the difference between the two excitation energies to the same state determined at not distant molecular geometries, we believe that the error due to neglect of electron correlation in the S_0 and T_1 states is not substantial. Using the vertical energies of Me^9T quoted in Table 2, the adiabatic energy of the T_1 state can be estimated to be 22,700 and 21,700 cm^{-1} in vacuo and ACN solution, respectively.

The emission spectrum of TI in an argon-saturated solution of ACN measured at room-temperature features a single band with a maximum at λ_{max} = 485 nm (Fig. 2). The excitation spectrum (not shown) of the 485 nm emission resembles that of the TI absorption. The emission is quenched by atmospheric oxygen (c_{O_2} = 1.9 mM in air-equilibrated ACN solution [29]) and by KI. The quenching by iodide obeyed Stern–Volmer kinetics, and the linear plot constructed from the measurements of the emission intensity ratios is shown as an inset in Fig. 2. Assuming that $k_q \approx k_{diff}$ (1.9×10^{10} M^{-1} s^{-1} in ACN [29]), the quenching indicates that the emission is long-lived (τ in the μs range) and was therefore ascribed to a $T_1 \rightarrow S_0$ phosphorescence. The phosphorescence can be attributed to the excited thione form of TI because Me^6TPR (Chart 1), the thioether derivative of TI, did not show a long-lived emission in this spectral region. The value of the phosphorescence quantum yield determined for the solution at the concentration c = 0.04 mM was very low ($\phi_p = 1 \times 10^{-4}$). The shape of the emission band (Fig. 2) is similar to that of the $^3(\pi\pi^*)$ phosphorescence of aromatic thioketones and exhibits only residual vibrational structure [42,43]. Therefore the energy of the T_1 state of TI could not be

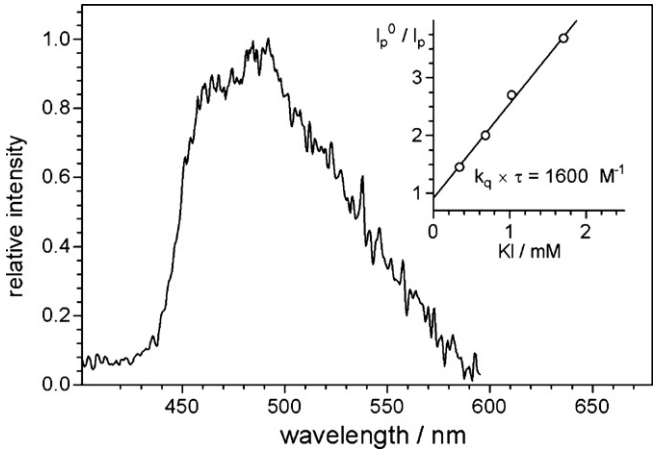

Fig. 2. Room-temperature emission spectrum of TI in argon–saturated ACN solution ($c_{TI} = 0.12 \times 10^{-4}$ M, λ_{exc} = 320 nm). Inset: the Stern–Volmer plot for the quenching of the emission by KI.

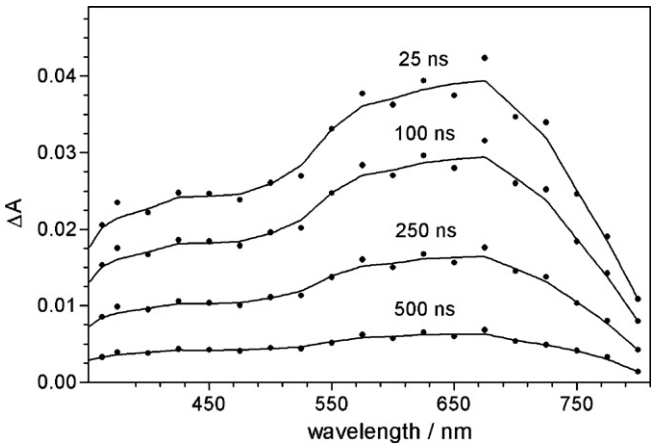

Fig. 3. Spectra of transient absorption recorded after excitation (λ_{exc} = 355 nm, 1 mJ) of an argon-saturated solution of TI in ACN ($c_{TI} = 0.8 \times 10^{-3}$ M) at various delay time.

accurately determined, and it was only roughly estimated from the position of a weakly marked shoulder located to the blue of the phosphorescence maximum. The estimated energy $E(T_1)$ (Table 3) is very close to the calculated energy for $T_1 \rightarrow S_0$ electronic transition (21,700 cm^{-1}, vide supra).

The transient absorption spectrum obtained by excitation (λ_{exc} = 355 nm) of an argon-saturated solution of TI in ACN is presented in Fig. 3. In the spectrum, an intense absorption with a maximum at λ = 675 nm and a weaker band in the spectral region 350–500 nm were observed. The transient absorption decay was independent of the monitoring wavelength and was accelerated in the presence of molecular oxygen and KI (Fig. 4). The quenching effect supports that the transient absorption originates from the TI excited T_1 state. The triplet–triplet absorption coefficient was determined using benzophenone as a standard (ε_T = 7220 M^{-1} cm^{-1}) [44,45] under the assumption that the quantum yield of the TI triplet state formation by intersystem crossing is ϕ_T = 1. This assumption is justified because, in general, the formation of the T_1 state in thiocarbonyl compounds, was found to be very efficient (e.g. TU, $\phi_T = 0.9 \pm 0.1$ in H_2O [1,12], and 6-thiopurine, ϕ_T = 0.99 in THF [46]). The value of ε_T = 3850 M^{-1} cm^{-1} at λ = 675 nm obtained for TI is similar to that reported for other N-heterocyclic thiocarbonyl compounds (ε_T = 6100 M^{-1} cm^{-1} at λ = 475 nm for 6-thiopurine in THF [46]; ε_T = 2400 M^{-1} cm^{-1} at λ = 540 nm for TU in H_2O [12,14]).

The $T_1 \rightarrow T_n$ transitions for the thione tautomer of Me^9TP were calculated at the CIS/aug-cc-pVTZ level of theory using the CPCM model for the ACN solvent, and the results are given in Supplementary material.

Table 3
Quantum yields and rate constants of the deactivation processes of the T_1 excited state of TI and TU in ACN solution.

	TI	TU
$E(T_1)$ [cm^{-1}][a]	22,000	20,500
ϕ^0_p	0.2×10^{-3}	2.5×10^{-3}
ϕ_{nr}	>0.99	>0.99
ϕ_{pch}	$<10^{-4}$[b]	0.008[c]
τ^0 [μs]	3.2	2.0
k_{sq} [M^{-1} s^{-1}]	7.4×10^9	5.1×10^9
k_p [s^{-1}]	60	1250
k_{nr} [s^{-1}]	$>3.1 \times 10^5$	$>4.9 \times 10^5$

[a]From phosphorescence spectrum; [b]substrate disappearance in argon-saturated solution at $c_{TI} = (1–5) \times 10^{-4}$ M, [c]substrate disappearance in argon-saturated solution at $c_{TU} = 5 \times 10^{-4}$ M, from ref. [48].

3.3. The T_1 excited state deactivation processes

3.3.1. Photophysical processes

Transient absorption spectroscopy was used for the study of the kinetics of the TI excited T_1 state decay. The rate of the transient absorption decay and, as a consequence, the excited T_1 state lifetime was found to be dependent on the solute concentration. This concentration dependence is characteristic of aliphatic and aromatic thiocarbonyl compounds. It is a result of a significant contribution from the self-quenching process to the deactivation of the T_1 state of the compounds [9–11,47]. The concentration independent, intrinsic lifetime, τ_T^0, was obtained from the $\lambda = 625$ nm transient absorption decay measurements performed for a series of argon-saturated solutions of TI at concentrations in the range of 0.1–1 mM. The experimentally measured lifetimes were analyzed according to the Stern–Volmer relation (Eq. (1))

$$1/\tau_T = 1/\tau_T^0 + k_{sq} \times c_{TI} \quad (1)$$

where τ_T is the experimental lifetime determined by a fitting of the $\lambda = 625$ nm absorbance decay with a single exponential function, k_{sq} is the self-quenching rate constant and c_{TI} is the concentration of TI in the solution. An example of an experimental transient absorption decay curve and a Stern–Volmer plot are displayed in Fig. 4. The values of τ_T^0 and k_{sq} derived from a linear plot of $1/\tau_T$ vs. c_{TI} are shown in Table 3.

Using the quantities: τ_T^0, k_{sq}, ϕ_p and the quantum yield of photochemical decay ϕ_{pch} (vide infra, Table 3) determined for TI in argon-saturated ACN solutions, the values of the phosphorescence quantum yield at infinite dilution (ϕ_p^0), the quantum yield of radiationless processes (ϕ_{nr}), radiative (k_p) and nonradiative (k_{nr}) rate constants were calculated from Eqs. (2)–(5). In the calculations, the quantum yield of T_1 formation in TI was assumed to be $\phi_T = 1$. The results are shown in Table 3.

$$\phi_p^0 = \phi_p \times (1 + k_{sq} \times \tau_T^0 \times c_{TI}) \quad (2)$$

$$k_p = \phi_p^0/\tau_T^0 \times \phi_T \quad (3)$$

$$\phi_{nr} = \phi_T - (\phi_p^0 + \phi_p^{ch}) \quad (4)$$

$$k_{nr} = \phi_{nr}/\tau_T^0 \times \phi_T \quad (5)$$

As follows from the results in Table 3, the radiative process is very slow, and it plays only a very minor role in the deactivation of the excited T_1 state of the investigated compound. This, in fact, could be expected because the T_1 excited state has a π,π^* configuration. In dilute solutions of TI ($c_{TI} \leq 0.01$ mM), the T_1 state decays

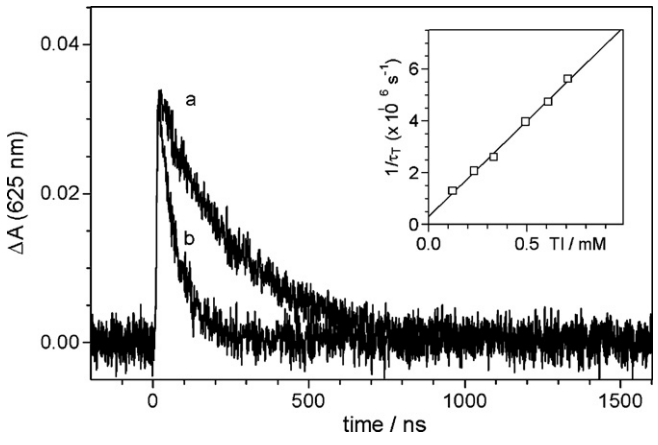

Fig. 4. Experimental traces of the 625 nm absorbance decay of TI: (a) in argon-saturated ($\tau_T = 248$ ns) and (b) air-equilibrated ($\tau_T = 52$ ns) ACN solution ($c_{TI} = 0.51 \times 10^{-3}$ M). Inset: Stern–Volmer plots of reciprocal of triplet lifetime ($1/\tau_T$) vs. concentration of TI in argon-saturated solution.

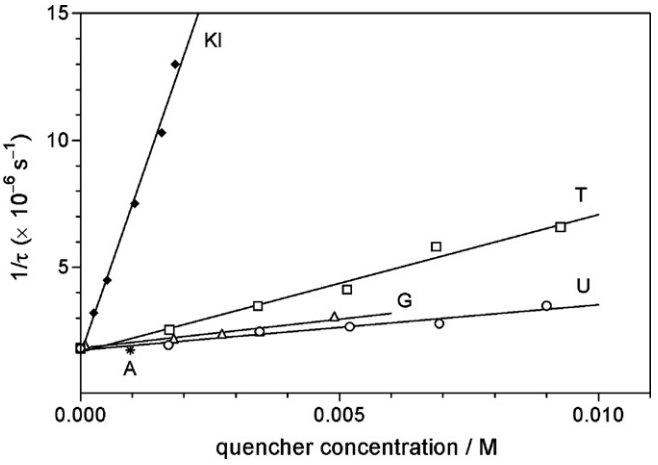

Fig. 5. Stern–Volmer plots of reciprocal of triplet lifetime ($1/\tau_T$) of TI vs. concentration of quenchers: 9-methyladenine (A), 2′,3′,5′-tri-O-acetyl-guanosine (G), 2′,3′,5′-tri-O-acetyl-uridine (U) and 3′,5′-di-O-acetyl-thymidine (T).

mainly through photophysical nonradiative processes, which can be either intramolecular or intermolecular (interaction with solvent molecules) [15]. Under these conditions less than 19% of all molecules in their T_1 state decay by self-quenching (i.e. the contribution of the s-q process to the overall decay of the TI molecules in the T_1 state equals to s-q (%) = 19%, calculated from Eq. (6)) [16]. In the concentration range $c_{TI} = 0.1$–0.5 mM the T_1 state decay is dominated by self-quenching (contribution from s-q = 70–92%), but apparently the interactions do not lead efficiently to stable photoproduct formation ($\phi_{pch} < 10^{-4}$, Table 3).

$$\text{contribution of s-q}\,(\%) = 100 \times (k_{sq} \times c_{TI})/(k_{sq} \times c_{TI} + 1/\tau_T^0) \quad (6)$$

As mentioned above, molecular oxygen and KI quench the T_1 state of TI. In addition, the presence of purine and pyrimidine derivatives (natural relatives of TI with respect to their incorporation into nucleic acids) was also found to accelerate the decay of the T_1 state of TI. In these latter quenching experiments 9-methyladenine and acetylated derivatives of guanosine, thymidine, uridine were used. They are denoted as A, G, T and U, respectively, in Fig. 5. In these experiments no formation of stable photoproducts could be detected by UV absorption spectroscopy of these solutions. In the presence of a quencher, the rate of the T_1 decay is described by Eq. (7)

$$1/\tau_T = 1/\tau_T^0 + k_{sq} \times c_{TI} + k_q \times c_q \quad (7)$$

For KI, as well as purine and pyrimidine quenchers, the bimolecular quenching rate constants (k_q) were determined from the linear dependence of the first-order rate constants of the T_1 state decay ($1/\tau_T$) on the concentration of quenchers (c_q) measured at a given concentration of TI ($c_{TI} = 0.26$ mM) (Fig. 5 and Table 4).

The k_q for quenching by O_2 was approximated from Eq. (7) using the experimental value of $1/\tau_T$ and previously determined quantities τ_T^0, k_{sq}, and the concentration of oxygen $c_{O_2} = 1.9$ mM (in air-equilibrated ACN) [29].

Table 4
The rate constants[a] ($k_q \times 10^{-9}$, [$M^{-1}\,s^{-1}$]) for the quenching of the T_1 state of TI in ACN solution.

O_2	KI[b]	A[b]	U[b]	G[b]	T[b]
6.8	5.9 (6.4)[c]	~0.2	0.18	0.25	0.54

[a]From transient absorption measurements; [b]in argon-saturated solution; [c]from phosphorescence quenching and $\tau_T = 2.5$ μs calculated from Eq. (1) for TI in solution at $c_{TI} = 0.12 \times 10^{-4}$ M.

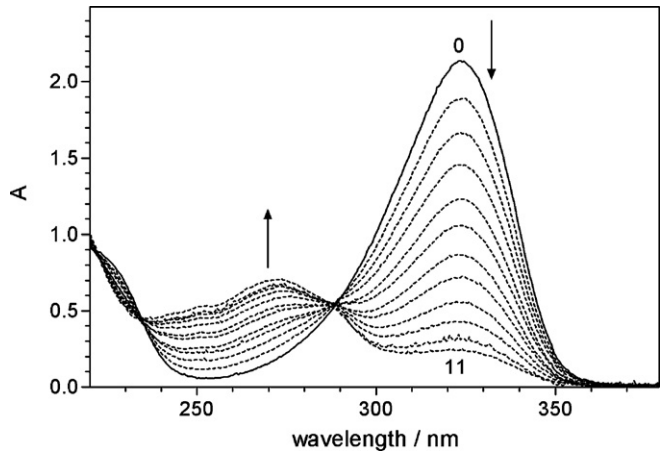

Fig. 6. UV absorption spectra of TI ($c = 1 \times 10^{-4}$ M) in air-equilibrated ACN before (solid line) and after irradiation at $\lambda = 313$ nm; spectra measured at time intervals of 1 min, the spectrum after 11 min corresponds to 87% conversion of substrate.

The quenching of the T_1 state of TI by O_2 and KI occur at very high rates, approaching the diffusion-controlled limit. The values of k_q for the purine and pyrimidine quenchers are all an order of magnitude lower, and, with the exception of thymidine (T), are very similar.

3.3.2. Steady state photochemistry

In contrast to the photostability of TI in argon-saturated ACN solutions in (Table 3), the photodecomposition of the compound is significantly enhanced ($\phi_{pch} = 0.014$) when irradiations were performed in the presence of atmospheric oxygen. T_1 is the reactive state since the subnanosecond lifetime of the singlet excited state makes its quenching unlikely at $c_{O_2} \leq 10^{-2}$ M. The sequential UV absorption spectra of TI upon $\lambda = 313$-nm irradiation are shown in Fig. 6. The spectral changes are compatible with the expectation that the thiocarbonyl group is engaged in the photoreaction. The reversed-phase HPLC analysis of the solution irradiated to ~50% conversion of the substrate reveals the presence of four major photoproducts (Scheme 1): peracetylated sulfinic acid (**1a**), sulfonic acid (**1b**), inosine (**2**) and disulfide (**3**). The photoproducts were formed with chemical yields (from HPLC) indicated in Scheme 1. They account for ~80% of the substrate consumed.

The photoproducts **1–3** were identified as described in Section 2.2.2. The photoproducts' concentration profiles (Supplementary material) showed that they all are present at very low substrate conversion. Therefore, they do not arise from the secondary photochemistry of a stable intermediate.

Oxygenated sulfur compounds, like sulfinic and sulfonic acids as well as the carbonyl analogs of the substrates have been previously reported to be the products of the photochemical oxygenation of a variety of heterocyclic compounds containing the thioimide function including 6-thiopurine [49–51] and TU [52,53]. These oxygenated sulfur products were suggested to arise from the reaction of thiocarbonyl compounds in the S_0 state with singlet oxygen $O_2(^1\Delta_g)$. This reactive oxygen species was produced in these reactions by an energy transfer from the excited T_1 state of the thiones to the ground state of the oxygen molecules [14,46,49–51]. Disulfides, however, have not been previously identified among the products of these photooxidation reactions.

Two possible reaction pathways were considered for the mechanism of the disulfide formation in the current work. Compound **3** could be formed by homolytic cleavage of an S—H bond, a typical primary photoreaction of thiols, followed by a combination of two sulfur centered (thiyl) radicals. However this route can be certainly ruled out, because both, theoretical and experimental results obtained in this work have given no evidence for the existence of a significant, detectable fraction of TI in its thiol form. The second mechanism relies on the fact that the formation of **3** requires the presence of oxygen. This would point to the involvement of an electron transfer process. Molecular oxygen is known to act as an electron acceptor whether it is in its ground state ($^3\Sigma_g^-$) or in its excited singlet state ($^1\Delta_g$) [54]. Both processes are presented below with the participation of TI in its T_1 excited state or in its ground state (S_0) (Eqs. (8) and (9), respectively).

$$TI(T_1) + O_2(^3\Sigma_g^-) \rightarrow TI^{\bullet+} + O_2^{\bullet-} \quad (8)$$

$$TI(S_0) + O_2(^1\Delta_g) \rightarrow TI^{\bullet+} + O_2^{\bullet-} \quad (9)$$

Of these two processes, only the one in Eq. (8) is feasible ($\Delta G < 0$) on thermodynamic grounds. The values of the free energy changes (ΔG) [29] were approximated from data available in the literature ($E(O_2/O_2^{\bullet-}) = -0.6$ V vs. NHE in DMF [14,55]; $E(TI^{\bullet+}/TI)$ approximated by the redox potential for thioinosine $E(TI^{\bullet+}/TI) = 0.24$ V vs. SCE [56], ≈0.5 V vs. NHE in H_2O, the T_1 excited state energy of TI, $\Delta E \approx 64$ kcal/mol in ACN (Table 3) and $\Delta E[O_2(^1\Delta_g)] = 22.6$ kcal/mol

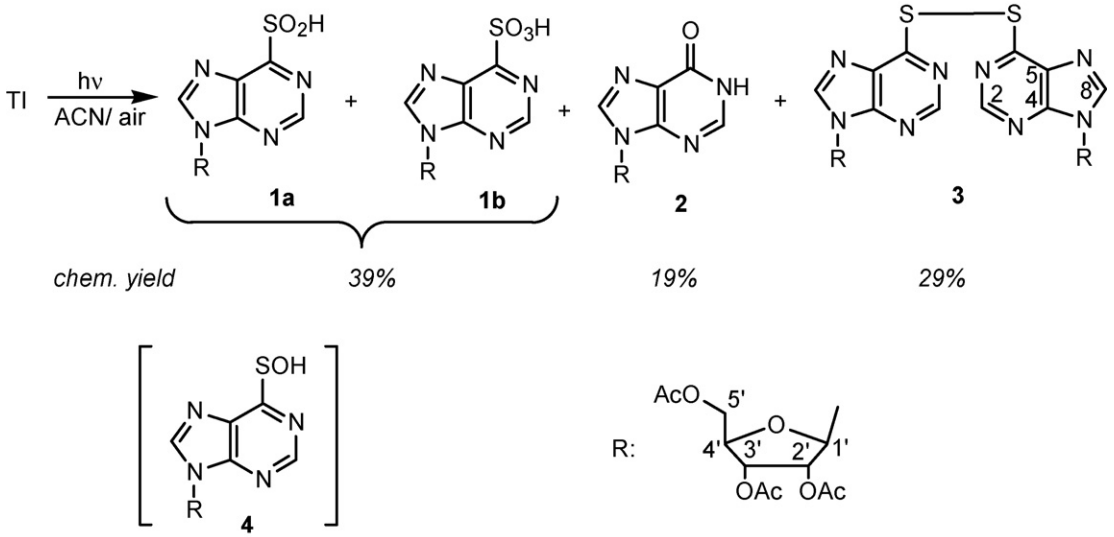

Scheme 1.

in organic solvents [57]). The results for the calculated free energy changes in the reactions are: $\Delta G \sim -39$ kcal/mol for (Eq. (8)) and $\Delta G \sim +3$ kcal/mol for (Eq. (9)).

Attempts were made to detect the products from an electron transfer reaction. In particular, evidence for the presence of the radical cation $TI^{\bullet+}$ was sought in transient absorption measurements. In these experiments, nitroblue tetrazolium [58] was used as an indicator to detect any presence of superoxide $O_2^{\bullet-}$. Neither experiment showed evidence for an electron transfer reaction.

On the other hand, the photoproducts **1**, **2** and **3** were found to be formed when methylene blue or rose bengal were used to generate O_2 ($^1\Delta_g$) in air-equilibrated ACN solution. In conclusion, it appears reasonable to postulate an unstable intermediate is involved in the production of the disulfide **3** from TI in the reaction with O_2 ($^1\Delta_g$). A sulfenic acid derivative of TI (**4**, Scheme 1) could be a likely candidate, as sulfenic acids are chemical oxidation products of a variety of thiols [59,60] and thioimides, including 9-methyl-6-thiopurine [61]. Guanine-6-sulfenate was also postulated as an unstable intermediate in the photooxidation of thioguanine [7]. The formation of disulfides from sulfenic acids (e.g. 2-pyridine-sulfenic acid [62]) has been reported [59,60].

4. Conclusions

Using combined experimental and quantum chemical approaches, the important parameters characterizing the T_1 state of TI in ACN solutions were determined. The thione form was found to be the exclusive tautomer of the compound in its S_0 state. The T_1 state of this tautomeric form was observed directly by room-temperature phosphorescence and nanosecond transient absorption spectroscopy. The T_1 (π,π^*) excited state of TI was characterized in terms of its phosphorescence, photochemical decay quantum yields, intrinsic lifetime, rate constants of the self-quenching, phosphorescence, nonradiative and radiative processes. Finally, it was of interest to compare the results obtained in this work for the thiopurine nucleoside (TI) with the parameters characterizing the T_1 (π,π^*) excited state of the thiopyrimidine nucleoside (TU, Chart 1). The data for TU are included in Table 3, and they were determined as described previously using ACN instead of carbon tertrachloride as a solvent [15,16]. As it can be seen from the information in Table 3, most of the parameters characterizing the two thione triplets are similar despite the significant structural differences between TI and TU (Chart 1). The notable differences between the two compounds refer to their phosphorescence and photochemical processes. The phosphorescence quantum yield of TI is an order of magnitude lower than that for TU. The photochemical decay of TI is a very inefficient process; the photochemical quantum yield of TI is about 100 times smaller than that for TU.

Acknowledgments

This work was performed under financial support of the Ministry of Science and Higher Education (MNiSW) Poland, project N N204 215434 for years 2008–2011. The authors thank Dr Gordon Hug for reading the manuscript and valuable comments. The calculations were performed at the Poznan Supercomputer Center (PCSS). The nanosecond transient absorption measurements were performed at Center for Ultrafast Laser Spectroscopy in Poznan.

Appendix A. Supplementary data

Supplementary data associated with this article can be found, in the online version, at doi:10.1016/j.jphotochem.2009.05.021.

References

[1] A. Favre, in: H. Morrison (Ed.), Bioorganic Photochemistry, J. Wiley & Sons, New York, 1990, pp. 379–425.
[2] A. Favre, C. Saintome, J. Fourrey, P. Clivio, P.A. Laugaa, J. Photochem. Photobiol. B: Biol. 42 (1998) 109–124.
[3] K. Meisenheimer, T. Koch, Crit. Rev. Biochem. Mol. Biol. 32 (1997) 101–140.
[4] J. Aarbakke, G. Janka-Schaub, G.B. Elion, Trends Pharmacol. Sci. 18 (1997) 3–7.
[5] A. Woisard, A. Favre, P. Clivio, J.-L. Fourrey, J. Am. Chem. Soc. 114 (1992) 10072–10074.
[6] C. Salet, M. Bazin, G. Moreno, A. Favre, Photochem. Photobiol. 41 (1985) 617–619.
[7] X. Zhang, G. Jeffs, X. Ren, P. O'Donovan, B. Montaner, C.M. Perrett, P. Karran, Y.-Z. Xu, DNA Repair 6 (2007) 344–354.
[8] A. Massey, Y.-Z. Xu, P. Karran, Curr. Biol. 11 (2001) 1142–1146.
[9] A. Maciejewski, R.P. Steer, Chem. Rev. 93 (1993) 67–98.
[10] A. Maciejewski, M. Szymanski, R.P. Steer, J. Phys. Chem. 92 (1988) 6939–6944.
[11] G. Burdziński, J. Kubicki, A. Maciejewski, R.P. Steer, S. Velate, E.K. Yeow, in: V. Ramamurthy, K. Schanze (Eds.), Organic Photochemistry and Photophysics, CRC, Taylor & Francis Group, Boca Raton, 2006, pp. 1–32.
[12] S.J. Milder, D.S. Klieger, J. Am. Chem. Soc. 107 (1985) 7365–7373.
[13] M.-R. Taherian, A.H. Maki, Chem. Phys. 55 (1981) 85–96.
[14] K. Heihoff, R.W. Redmond, S.E. Braslavsky, M. Rougee, C. Salet, A. Favre, R.V. Benssason, Photochem. Photobiol. 51 (1990) 635–641.
[15] K. Taras-Goślinska, G. Wenska, B. Skalski, A. Maciejewski, G. Burdzinski, J. Karolczak, Photochem. Photobiol. 75 (2002) 448–456.
[16] K. Taras-Goślińska, G. Wenska, B. Skalski, A. Maciejewski, G. Burdzinski, J. Photochem. Photobiol. A: Chem. 168 (2004) 227–233.
[17] Y. Harada, T. Suzuki, T. Ichimura, Y.-Z. Xu, J. Phys. Chem. B 111 (2007) 5518–5524.
[18] Y. Rubin, Y. Morozov, D. Vankateswarlu, J. Leszczyński, J. Phys. Chem. A 102 (1998) 2194–2200.
[19] M.K. Shukla, J. Leszczynski, J. Phys. Chem. A 108 (2004) 10367–10375.
[20] H. Bredereck, A. Martini, Chem. Ber. 80 (1947) 401–405.
[21] J. Zemlicka, J. Smrt, F. Sorm, Collect. Czech. Chem. Commun. 29 (1964) 635–643.
[22] R.K. Robins, J. Am. Chem. Soc. 79 (1957) 490–494.
[23] J. Fox, D. Van Praag, I. Wempen, I.L. Doerr, L.X. Cheong, J.E. Knoll, M.L. Eidinoff, A. Bendich, G.B. Brown, J. Am. Chem. Soc. 81 (1959) 178–187.
[24] J. Fox, I. Wempen, A. Hampton, I.L. Doerr, J. Am. Chem. Soc. 80 (1958) 1669–1675.
[25] J.F. Gerster, J.W. Jones, R.K. Robins, J. Org. Chem. 28 (1963) 945–948.
[26] W.H. Miller, R.O. Roblin Jr., E.B. Astwood, J. Am. Chem. Soc. 67 (1945) 2201–2204.
[27] R.S. Meech, D. Phillips, J. Photochem. 23 (1983) 193–217.
[28] I.L. Doerr, I. Wempen, D.A. Clarke, J.J. Fox, J. Org. Chem. 26 (1961) 3401–3409.
[29] S.L. Murov, I. Carmichael, G.L. Hug, Handbook of Photochemistry, second ed., Marcel Dekker, New York, 1993.
[30] G. Burdzinski, A. Maciejewski, G. Buntinx, O. Poizat, C. Lefumeux, Chem. Phys. Lett. 384 (2004) 332–338.
[31] C. Møller, M.S. Plesset, Phys. Rev. 46 (1934) 618–622.
[32] T.H. Dunning Jr., J. Chem. Phys. 90 (1989) 1007–1023.
[33] R.A. Kendall, T.H. Dunning Jr., R.J. Harrison, J. Chem. Phys. 96 (1992) 6796–6806.
[34] K. Raghavachari, G.W. Trucks, J.A. Pople, M. Head-Gordon, Chem. Phys. Lett. 157 (1989) 479–483.
[35] J.B. Foresman, M. Head-Gordon, J.A. Pople, M.J. Frisch, J. Phys. Chem. 96 (1992) 135–149.
[36] M. Head-Gordon, R.J. Rico, M. Oumi, T.J. Lee, Chem. Phys. Lett. 219 (1994) 21–29.
[37] V. Barone, M. Cossi, J. Phys. Chem. A 102 (1998) 1995–2001.
[38] M.J. Frisch, G.W. Trucks, H.B. Schlegel, G.E. Scuseria, M.A. Robb, J.R. Cheeseman, J.A. Montgomery Jr., T. Vreven, K.N. Kudin, J.C. Burant, J.M. Millam, S.S. Iyengar, J. Tomasi, V. Barone, B. Mennucci, M. Cossi, G. Scalmani, N. Rega, G.A. Petersson, H. Nakatsuji, M. Hada, M. Ehara, K. Toyota, R. Fukuda, J. Hasegawa, M. Ishida, T. Nakajima, Y. Honda, O. Kitao, H. Nakai, M. Klene, X. Li, J.E. Knox, H.P. Hratchian, J.B. Cross, C. Adamo, J. Jaramillo, R. Gomperts, R.E. Stratmann, O. Yazyev, A.J. Austin, R. Cammi, C. Pomelli, J.W. Ochterski, P.Y. Ayala, K. Morokuma, G.A. Voth, P. Salvador, J.J. Dannenberg, V.G. Zakrzewski, S. Dapprich, A.D. Daniels, M.C. Strain, O. Farkas, D.K. Malick, A.D. Rabuck, K. Raghavachari, J.B. Foresman, J.V. Ortiz, Q. Cui, A.G. Baboul, S. Clifford, J. Cioslowski, B.B. Stefanov, G. Liu, A. Liashenko, P. Piskorz, I. Komaromi, R.L. Martin, D.J. Fox, T. Keith, M.A. Al-Laham, C.Y. Peng, A. Nanayakkara, M. Challacombe, P.M.V. Gill, B. Johnson, W. Chen, M.W. Wong, C. Gonzales, J.A. Pople, Gaussian 03, revision D.01, Gaussian, Inc., Pittsburgh, PA, 2003.
[39] L. Lapiński, M.J. Nowak, J.S. Kwiatkowski, J. Leszczyński, J. Phys. Chem. A 103 (1999) 280–288.
[40] M. El Sayed, J. Chem. Phys. 38 (1963) 2834–2838.
[41] A. Maciejewski, M. Szymanski, R.P. Steer, J. Phys. Chem. 90 (1986) 6314–6318.
[42] A. Maciejewski, M. Szymanski, R.P. Steer, Chem. Phys. Lett. 143 (1988) 559–564.
[43] M. Milewski, J. Baksalary, P. Antkowiak, W. Augustyniak, M. Binkowski, J. Karolczak, D. Komar, A. Maciejewski, M. Szymanski, W. Urjasz, J. Fluoresc. 10 (2000) 89–97.
[44] C.V. Kumar, L. Qin, P.K. Das, J. Chem. Soc. Faraday Trans. 2 80 (1984) 783–793.
[45] A.A. Lamola, G.S. Hammond, J. Chem. Phys. 43 (1965) 2129–2135.
[46] M.M. Alam, M. Fujitsuka, A. Watanabe, O. Ito, J. Phys. Chem. A 102 (1998) 1338–1344.
[47] U. Brühlmann, J.R. Huber, Chem. Phys. Lett. 54 (1978) 606–610.
[48] K. Taras-Goślińska, G. Wenska, B. Skalski, Annales, Facultatis Chemiae, Universitatis, Studiorum Mickiewicziane Posnaniensis 2 (2002) 255–261.
[49] V.J. Hemmens, D.E. Moore, J. Chem. Soc. Perkin Trans. 2 (1984) 209–211.
[50] V.J. Hemmens, D.E. Moore, Photochem. Photobiol. 43 (1986) 247–255.

[51] G. Wenska, S. Paszyc, Z. Naturforsch. 36b (1981) 1628–1631.
[52] H. Ochiai, H. Shibata, J. Agric. Soc. Jpn. 48 (1974) 643–649.
[53] M. Pleiss, H. Ochiai, P.A. Cerutti, Biochem. Biophys. Res. Commun. 34 (1969) 70–76.
[54] R.V. Bensasson, E.J. Land, T.G. Truscott, Excited States and Free Radicals in Biology and Medicine, Oxford University Press Inc., New York, 1993, p. 150.
[55] D.T. Sawyer, G. Chiericato, C.T. Angelis, E.J. Nanni, T. Tsuchiya, Anal. Chem. 54 (1982) 1720–1724.
[56] R.N. Goyal, A. Rastogi, A. Sangal, New J. Chem. 25 (2001) 545–550.
[57] W.D.K. Clark, C. Steel, J. Am. Chem. Soc. 93 (1971) 6347–6355.
[58] K. Umemoto, N. Okamura, Bull. Chem. Soc. Jpn. 59 (1986) 3047–3052.
[59] F.A. Davis, R.L. Billmers, J. Am. Chem. Soc. 103 (1981) 7016–7018.
[60] T. Fekner, J.E. Baldwin, R.M. Adlington, C.J. Schofield, Tetr. Lett. 39 (1998) 6983–6986.
[61] T.T. Abraham, L.M. Benson, I. Jardine, J. Med. Chem. 26 (1983) 1523–1526.
[62] F.A. Davies, R.H. Jenkins Jr., J. Am. Chem. Soc. 102 (1980) 7967–7969.